

See discussions, stats, and author profiles for this publication at: <https://www.researchgate.net/publication/231697824>

# Synthesis of Poly(arylene ether) Copolymers Containing Pendant PEO Groups and Evaluation of Their Blends as Proton Conductive Membranes

ARTICLE *in* MACROMOLECULES · OCTOBER 2005

Impact Factor: 5.8 · DOI: 10.1021/ma050615m

---

CITATIONS

18

---

READS

36

## 2 AUTHORS:



[Valadoula A. Deimede](#)

University of Patras

31 PUBLICATIONS 725 CITATIONS

SEE PROFILE



[Joannis K. Kallitsis](#)

University of Patras

196 PUBLICATIONS 4,027 CITATIONS

SEE PROFILE

# Synthesis of Poly(arylene ether) Copolymers Containing Pendant PEO Groups and Evaluation of Their Blends as Proton Conductive Membranes

Valadoulia A. Deimede\* and Joannis K. Kallitsis

Department of Chemistry, University of Patras, G.R.-26500 Patras, Greece, and Foundation of Research and Technology-Hellas (FORTH), Institute of Chemical Engineering and High-Temperature Chemical Processes (ICE-HT), P.O. Box 1414, G.R.-26500 Patras, Greece

Received March 23, 2005; Revised Manuscript Received September 15, 2005

**ABSTRACT:** A new series of poly(arylene ether) copolymers containing pendant poly(ethylene oxide) (PEO) groups are presented. Copolymers were prepared via potassium carbonate mediated direct aromatic nucleophilic substitution polycondensation of dihydroxy end-functionalized PEO, bisphenol A, and 4-fluorophenyl sulfone or decafluorobiphenyl. The obtained copolymers (PAE-*g*-PEO and FPAE-*g*-PEO) showed excellent film-forming properties, high thermal stability, and glass transition temperatures up to 110 °C. This polymeric structure resulted in amorphous copolymers in most cases, a main requirement for high ionic conductivity of solid polymer electrolytes. The incorporation of the hydrophilic PEO units in the hydrophobic aromatic polyether backbone improved the water uptake ability, producing in some cases water-soluble polymers. Blends of sulfonated polysulfone and water-soluble poly(ether sulfone) containing PEO side chains (PES-*g*-PEO) were also studied in terms of fuel cell relevant parameters like thermal behavior, water uptake, morphology, and ionic conductivity. Flexible membranes prepared by casting showed high glass transition temperatures up to 215 °C. SEM images of blend membranes revealed the existence of hydrophilic spherical domains with average sizes of 50–100 nm. The water uptake ability of the membranes increased with increasing PES-*g*-PEO content and temperature, and proton conductivity values were measured in the range of  $10^{-3}$  S/cm at room temperature and relative humidity 65%. The above results demonstrate that these materials could be applied as polymer electrolytes in proton exchange membrane fuel cells (PEMFC).

## Introduction

Proton exchange membrane fuel cells (PEMFC)s are promising clean power sources for vehicular transportation and domestic applications.<sup>1</sup> As one of the key components of the membrane electrode assembly (MEA), proton exchange membranes (PEM) support the catalyst, provide ionic pathways for protons, and prevent crossover of gases or fuel. At present, sulfonated perfluoropolymers such as DuPont's Nafion have been almost the only advanced membranes that are used in practical systems due to their high proton conductivity, good mechanical strength, and high thermal and chemical stability. However, there are few drawbacks including high cost, low conductivity at low humidity or high temperatures, and high methanol permeability which seriously limit their application. Thus, the development of alternative materials overcoming these problems is strongly desired.

All existing membrane materials for low-temperature PEM fuel cells rely on absorbed water and its interaction with acid groups which act as proton exchange sites to facilitate ionic conductivity. Thus, an effective approach is the acid functionalization of wholly aromatic polymers which are thought to be one of the most promising routes to high-performance PEMs. This is due to their commercial availability, processability, wide variety of chemical compositions, and well-known oxidative and hydrolytic stability in the fuel cell environment.<sup>2</sup> Specifically, sulfonated poly(arylene ether) materials such as sulfonated poly(arylene ether ether

ketone) (SPEEK),<sup>3–7</sup> sulfonated poly(arylene ether sulfone),<sup>8–12</sup> and their derivatives are the focus of many investigations. One of the critical issues is the morphology of the sulfonated polymer membranes, which is controlled by the nanophase separation between hydrophobic and hydrophilic domains. The hydrophobic domains provide the polymers with morphological stability while the hydrophilic ones are responsible for ion conduction.

An alternative approach for the development of proton conductive materials is the incorporation of hydrophilic poly(ethylene oxide) units onto a stiff polymer backbone. Poly(ethylene oxide) (PEO)-based polymeric electrolytes are still among the most extensively studied polymeric conductors since their structures are beneficial for supporting fast ion transport.<sup>13</sup> A main drawback is the high crystallinity which limits the high ionic conductivity of PEO-based electrolytes.<sup>14–17</sup> Efforts to enhance the ionic conductivity of PEO-based electrolytes have focused on suppressing its crystallinity by the use of polymer architectures where short PEO chains are attached as pendant chains to backbone polymers,<sup>18–21</sup> incorporated in block copolymers,<sup>22,23</sup> or blended with other polymers<sup>24–26</sup> in which PEO forms the conductive phase and the other component acts as a mechanical support.

In the present work, poly(arylene ether)s containing PEO side chains (MW = 2000, 5000) with different weight fractions (8–95%) have been synthesized as candidate polymer electrolyte materials for proton exchange membrane (PEM) fuel cells. The obtained polymers show good thermal stability, very good mechanical and film-forming properties, and relatively

\* To whom correspondence should be addressed: Ph +302610-965248; Fax +302610-997122; e-mail deimede@iceht.forth.gr.

high water uptake. Blends composed of sulfonated polysulfone and PEO-*g*-PES in different compositions have also been prepared. These blends exhibit very good mechanical properties, very high water uptake, and high ionic conductivity ( $4 \times 10^{-3}$  S/cm) at ambient temperatures.

## Experimental Part

**Materials.** 4-Fluorophenyl sulfone (DFDPS), 2,2-bis(4-hydroxyphenyl)propane, and decafluorobiphenyl (DFB) were obtained from Aldrich Chemical Co. *N,N*-Dimethylformamide (DMF), *N,N*-dimethylacetamide (DMA), toluene, methanol, dichloromethane, chloroform, and diethyl ether were obtained from commercial sources and used as received. Anhydrous potassium carbonate was dried at 60 °C for 10 h in a vacuum oven. Dihydroxy-PEO 2000 and dihydroxy-PEO 5000 were synthesized as described elsewhere.<sup>27</sup> Sulfonated polysulfone in the sodium salt form (SPSF(Na)) was prepared according to known procedures.<sup>8,28</sup> The sulfonation degree determined by <sup>1</sup>H NMR was 55%.

**Synthesis of PEO-Based Poly(arylene ether)s. (a) Synthesis of Polymer PES-*g*-PEO-1.** A typical polymerization procedure is as follows. To a 10 mL, three-neck flask equipped with a magnetic stirrer, a Dean-Stark trap, and an argon gas inlet, dihydroxy-PEO 5000 (0.4635 g, 0.09 mmol), 4-fluorophenyl sulfone (0.0229 g, 0.09 mmol), potassium carbonate (0.0186 g, 0.13 mmol) in 3 mL of DMF, and 2.1 mL of toluene were added under an argon atmosphere. The reaction mixture was heated to 160–170 °C and maintained at this temperature for 20 h. The reaction mixture was diluted with DMF (5 mL) and poured slowly into a large excess of diethyl ether. The precipitated polymer was filtered and washed several times with diethyl ether. The polymer obtained was redissolved in 20 mL of chloroform and poured slowly in a large excess of diethyl ether with stirring. The polymer was precipitated out, filtered, washed with diethyl ether, and dried at 50 °C under vacuum for 24 h.

**(b) Synthesis of Polymer PES-*g*-PEO-2.** Polymer PES-*g*-PEO-2 was synthesized from dihydroxy-PEO 2000 and 4-fluorophenyl sulfone using the same procedure as the synthesis of polymer PES-*g*-PEO-1.

**(c) Synthesis of Copolymer PAE-*g*-PEO-3.** A typical polymerization procedure for copolymer PAE-*g*-PEO-3i is as follows. Dihydroxy-PEO 2000 (0.1290 g, 0.06 mmol), 2,2-bis(4-hydroxyphenyl)propane (bisphenol A) (0.2145 g, 0.94 mmol), 4-fluorophenyl sulfone (0.2542 g, 1.00 mmol), potassium carbonate (0.2070 g, 1.50 mmol), and 0.7 mL of DMF and 0.45 mL of toluene were introduced into a 10 mL, three-neck, round-bottom flask equipped with a magnetic stirrer, a Dean-Stark trap, and an argon inlet. The reaction mixture was heated to 160–170 °C for 20 h. The viscous mixture was diluted with 5 mL of DMF and was poured into a large excess of MeOH/H<sub>2</sub>O mixture 2/1, where a white polymer was precipitated. The solid was washed several times with water (to remove the inorganic impurities) and methanol and then was redissolved with dichloromethane and again poured into a large excess of MeOH/H<sub>2</sub>O mixture 2/1. The precipitated polymer was filtered, washed with methanol and water, and dried under vacuum at 50 °C for 24 h.

**(d) Synthesis of Copolymer FPAE-*g*-PEO-4.** Dihydroxy-PEO 2000 (0.1290 g, 0.06 mmol), 2,2-bis(4-hydroxyphenyl)propane (bisphenol A) (0.2145 g, 0.94 mmol), decafluorobiphenyl (0.3341 g, 1.00 mmol), potassium carbonate (0.2070 g, 1.50 mmol), and 1.5 mL of DMA were introduced into a 10 mL, three-neck, round-bottom flask equipped with a magnetic stirrer, a Dean-Stark trap, and an argon inlet. The reaction mixture was heated at 150–155 °C for 24 h. The viscous reaction mixture was diluted with DMA (5 mL), and after cooling to room temperature, the solution was poured into a large amount of methanol. The precipitated polymer was filtered and stirred overnight in water to remove the inorganic impurities. The polymer was filtered and washed with water and hexane. Finally, it was dissolved in dichloromethane

filtered and poured into a large amount of methanol in order to obtain a white polymer. The precipitated polymer was filtered, washed with methanol, and dried under vacuum at 50 °C.

**Characterization.** <sup>1</sup>H NMR spectra were obtained on a Bruker Advance DPX 400 MHz spectrometer. The samples were dissolved in either deuterated chloroform (CDCl<sub>3</sub>) or deuterated dimethyl sulfoxide (*d*<sub>6</sub>-DMSO).

Gel permeation chromatography (GPC) measurements were carried out using a Polymer lab chromatograph equipped with two Ultra Styragel columns (10<sup>4</sup>, 500 Å), UV detector (254 nm), and CHCl<sub>3</sub> as eluent, at 25 °C with a flow rate of 1 mL/min.

**Thermal Properties.** DMA measurements were conducted using a solid-state analyzer RSA II, Rheometrics Scientific Ltd., at 10 Hz.

Thermogravimetric analysis (TGA) was performed on a TA Instruments thermogravimetric analyzer model Q50. The samples were heated at 10 °C/min to 800 °C under an argon atmosphere.

Differential scanning calorimetry (DSC) measurements were conducted on a TA Instruments model DSC Q100 series. The heating and cooling runs were conducted at a rate of 10 °C min<sup>-1</sup> for all the measurements.

**SEM Studies.** Membrane morphology was studied by scanning electron microscopy (SEM) using a LEO Supra 35VP microscope. Solution-cast samples were cryo-fractured at liquid nitrogen temperature. The sample surfaces were coated with a thin layer of gold before examination.

**Determination of Water Uptake.** The membranes were dried under vacuum at 90 °C for 3 days, weighted, and then immersed in distilled water for 24 h at determined temperatures. Surface attached water was quickly removed with tissue paper and the weight of the wet membrane determined. The water uptake content can be calculated by

$$\text{uptake content (\%)} = \frac{\omega_{\text{wet}} - \omega_{\text{dry}}}{\omega_{\text{dry}}} \times 100\%$$

where  $\omega_{\text{wet}}$  and  $\omega_{\text{dry}}$  are the masses of wet and dried samples, respectively.

**Proton Conductivity Measurements.** All measurements were conducted at a conductivity four-probe cell at room temperature. The cell with the hydrated membrane was placed inside a humidified vessel in order to control the relative humidity by passing through the cell a mixture of humidified and dry nitrogen. The relative humidity values were confirmed by a hygrometer. Conductivity measurements were carried out by the current interruption method using a potentiostat/galvanostat (EG and G model 273) and an oscillator (Hitachi model V-650F).

**Membrane Preparation of Polymers PAE-*g*-PEO-3 and FPAE-*g*-PEO-4.** An amount of 0.15 g of polymer was dissolved in 15 mL of dichloromethane and filtered. The filtered solution was poured onto a glass plate, and the solvent was removed slowly at room temperature. The obtained membranes were dried under vacuum at 50 °C for 24 h.

**Membrane Preparation of Polymer Blends (SPSF-(Na)<sub>55</sub>/PES-*g*-PEO).** Blends were prepared by dissolving sulfonated polysulfone with sulfonation degree 55% (SPSF-(Na)<sub>55</sub>) and PES-*g*-PEO-1ii in DMF (5% w/v) at different ratios and poured onto a glass plate at 85 °C in an oven for 20 h. Homogeneous, transparent films with good mechanical properties were obtained. To remove any excess of the solvent, the membranes were dried under vacuum at 90 °C for 3 days. The studied blends are given in Table 3.

## Results and Discussion

Our synthetic strategy was based on the incorporation of PEO functionalities onto an aromatic polyether backbone to combine their ability to retain water molecules and subsequently give high ionic conductivity, with the good mechanical properties of the aromatic backbone. Dihydroxy end-functionalized PEO and bisphenol A were copolymerized with 4-fluorophenyl sulfone to yield aromatic polyethers containing pendant PEO groups.

Table 1. Syntheses of PEO-Based Poly(arylene ether)s

polymers	monomers molar ratio					
	DFDPS	PEO diol ( $M_n = 2000$ )	PEO diol ( $M_n = 5000$ )	bisphenol A	DFB	PEO content (wt %)
PES-g-PEO-1i	1		1			95.5
PES-g-PEO-1ii	1		1			95.5
PES-g-PEO-2i	1	1				89.4
PAE-g-PEO-3i	1	0.02		0.98		8.2
PAE-g-PEO-3ii	1	0.06		0.94		21.6
PAE-g-PEO-3iii	1	0.1		0.9		31.9
FPAE-g-PEO-4		0.06		0.94	1	19.0

Table 2. Molecular Weights of Polymers Determined by GPC

polymers	GPC ( $\text{CHCl}_3$ )		
	$M_n$	$M_w$	PDI
PES-g-PEO-1i	10 000	23 600	2.4
PES-g-PEO-1ii	21 300	42 600	2.0
PES-g-PEO-2i	14 600	33 400	2.3
PAE-g-PEO-3i	33 700	77 300	2.3
PAE-g-PEO-3ii	42 800	131 300	3.1
PAE-g-PEO-3iii	58 600	150 200	2.6
FPAE-g-PEO-4	36 900	122 600	3.3

Table 3. Water Uptake of the Copolymers PAE-g-PEO and FPAE-g-PEO

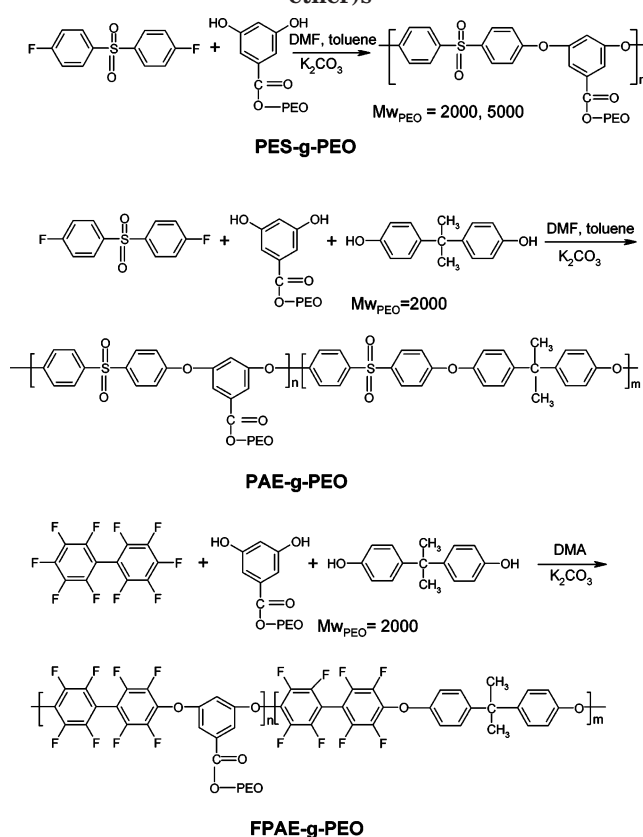
polymers	water uptake (%) <sup>a</sup>		
	20 °C	70 °C	100 °C
PAE-g-PEO-3i	0	7	12
PAE-g-PEO-3ii	0	10	13
PAE-g-PEO-3iii	34	40	49
FPAE-g-PEO-4	0	0	1

<sup>a</sup> Conducted at the desired temperatures for 24 h.

This copolymerization approach was mainly used to disrupt the regular structure and decrease crystallinity of PEO, while using an aromatic polyether backbone, poly(arylene ether)s substituted with PEO side chains with excellent mechanical properties were synthesized.

All polymers were prepared by  $\text{K}_2\text{CO}_3$ -mediated direct nucleophilic substitution polycondensation, as shown in Scheme 1. First, polymerization of PEO diol ( $MW = 2000$  or  $MW = 5000$ ) and 4-fluorophenyl sulfone (DFDPS) in equivalent molar ratio in DMF and toluene resulted in polymers (PES-g-PEO) with moderate molecular weights (Table 1). The obtained polymers are very soluble in common solvents like chloroform, DMF, and dimethyl sulfoxide. These are also soluble in water, a property that is not desirable. Therefore, these polymers cannot be used directly as polymer electrolyte membranes. Since a critical factor for the synthesis of proper polymeric electrolyte membranes is the interplay between hydrophobicity and hydrophilicity, copolymerization of hydrophilic and hydrophobic monomers is a practical approach. Thus, copolymers PAE-g-PEO with different PEO diol molar percentage were synthesized by varying the feed ratio of PEO diol monomer to bisphenol A diol monomer. PAE-g-PEO-3 copolymers were synthesized using 4-fluorophenyl sulfone monomer, while FPAE-g-PEO-4 copolymer was synthesized using decafluorobiphenyl monomer. Polymerization conditions and details of the resulting polymers are given in Table 1. High molecular weights copolymers were obtained with number-average molar mass between 30 000 and 60 000 (Table 2), as determined by GPC with PS standards. However, it should be noted that calibration with polystyrene standards underestimates the number-average molar mass of short chain PEGs.<sup>29</sup> The

Scheme 1. Synthesis of PEO-Based Poly(arylene ether)s



synthesized copolymers are very soluble in common solvents such as dichloromethane, chloroform, and dimethyl sulfoxide. All copolymers were successfully cast into transparent and flexible membrane films with excellent mechanical properties using dichloromethane, indicating also the high molecular weights of the polymers. Copolymer PAE-g-PEO-3iii, which has the higher PEO weight percentage (31.9%), can form only brittle films.

The molecular structures of copolymers were confirmed by  $^1\text{H}$  NMR. The  $^1\text{H}$  NMR spectrum of copolymer PAE-g-PEO-3ii in deuterated chloroform with the assignment of the peaks is given in Figure 1.

In particular, the two doublet peaks centered at 7.85 and 7.00 ppm were ascribed to the aromatic protons of oxy-1,4-phenylenesulfone, while the doublet ones at around 6.95 and 7.25 ppm were assigned to bisphenol and 3,5-oxyphenylene PEO moieties. The signal at 3.6 ppm was attributed to oxyethylene hydrogens of PEO. Information about the copolymer composition was obtained from calculations based on the ratio of integrated peak intensities in the region around 6.90–7.85 ppm ascribed to the aromatic protons and at 3.6 ppm corresponding to the methylene protons of the EO backbone.



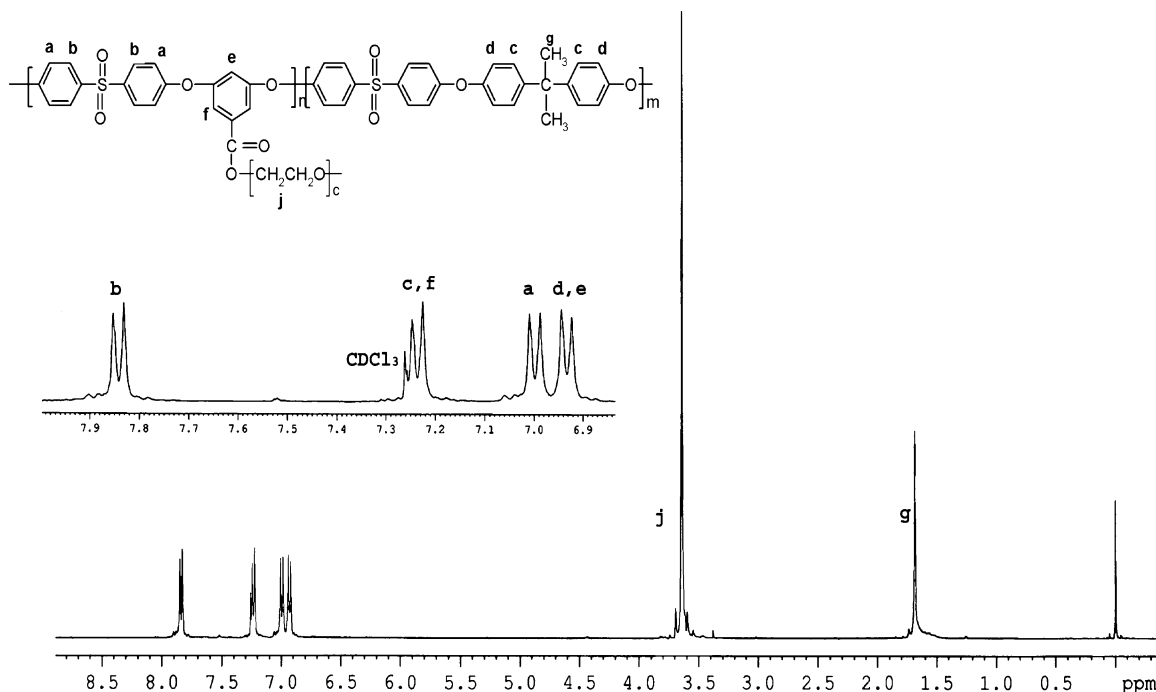


**Figure 1.**  $^1\text{H}$  NMR spectrum of copolymer **PAE-g-PEO-3ii** with the assignment of the peaks. The inset shows the aromatic region in an enlarged scale.

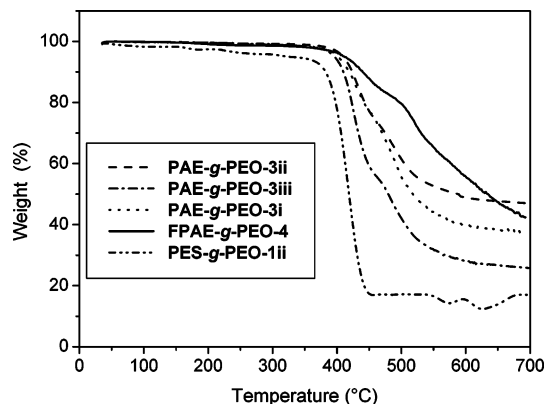


**Figure 2.** TGA traces of polymers **PES-g-PEO-1**, **PAE-g-PEO-3**, and **FPAE-g-PEO-4** under an argon atmosphere.

The calculated copolymer compositions were in good agreement with the composition of the monomer feed ratio from the copolymerization reactions.

Thermal stabilities of the synthesized polymers were investigated by TGA at a heating rate of  $10\text{ }^\circ\text{C}/\text{min}$  under an argon atmosphere. TGA curves of copolymers with different PEO weight fractions are given in Figure 2. Copolymers **PAE-g-PEO-3i-3iii** with PEO weight fraction between 8.2 and 31.9% showed better thermal stability than **PES-g-PEO-1ii** polymer, which had only one weight loss step with an onset at around  $360\text{ }^\circ\text{C}$ , corresponding to the loss of PEO groups and degradation of the polymer backbone. In the case of copolymers **PAE-g-PEO-3i-3iii** and **FPAE-g-PEO-4**, a distinct two-step degradation process was discernible. These copolymers revealed excellent thermal stability, with an onset of the first major weight loss at about  $380\text{ }^\circ\text{C}$  (loss of the PEO groups) and a 5% weight loss at around  $400\text{ }^\circ\text{C}$ . The second major weight loss begun at around  $450\text{ }^\circ\text{C}$  for copolymers **PAE-g-PEO-3i-3iii** and **FPAE-g-PEO-4**, corresponding to the decomposition of the poly(arylene ether) backbone. Copolymer **PAE-g-PEO-3iii** with the highest PEO weight fraction (31.9%) showed

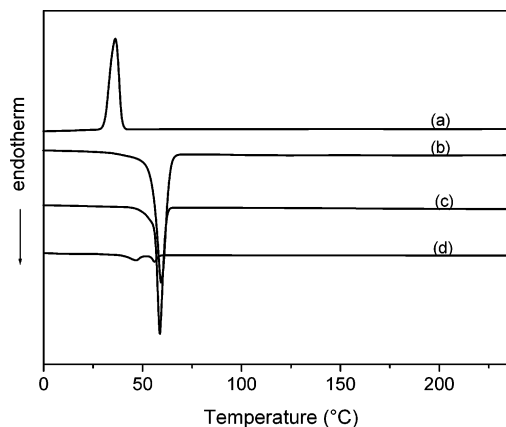


**Figure 3.** DSC thermograms for polymer **PES-g-PEO-1ii** (a) first cooling scan, (b) first heating scan, (c) second heating scan, and **PAE-g-PEO-3iii** (d) first heating scan.

a higher weight loss of about 40% at  $450\text{ }^\circ\text{C}$ , compared to that of the corresponding copolymers with weight fraction 8.2 and 21.6%, respectively.

Copolymer **FPAE-g-PEO-4**, which has a fluoro aryl ether backbone, exhibited higher thermal stability. Despite the fact that it contains almost the same amount of PEO with copolymer **PAE-g-PEO-3ii**, it is more thermally stable, showing slower decomposition rates both in the first and second decomposition steps.

Thermal properties of the copolymers films cast from dichloromethane solution were examined by using DSC. Typical thermograms of polymer **PES-g-PEO-1ii** and copolymer **PAE-g-PEO-3iii** are given in Figure 3. Polymer **PES-g-PEO-1ii** had an endothermic at  $59\text{ }^\circ\text{C}$  (at the first and second heating scan) and also an exothermic peak at  $32\text{ }^\circ\text{C}$ , from polyether (PEO, MW = 5000) melting and crystallization, respectively. Copolymer **PAE-g-PEO-3iii** with PEO weight content of 31.9% exhibited two endothermic peaks at 47 and  $55\text{ }^\circ\text{C}$  only at the first heating scan.<sup>30</sup>  $T_m$  of pure PEO with a molecular weight of 2000 is known to be  $\sim 54\text{ }^\circ\text{C}$ .<sup>31</sup> The

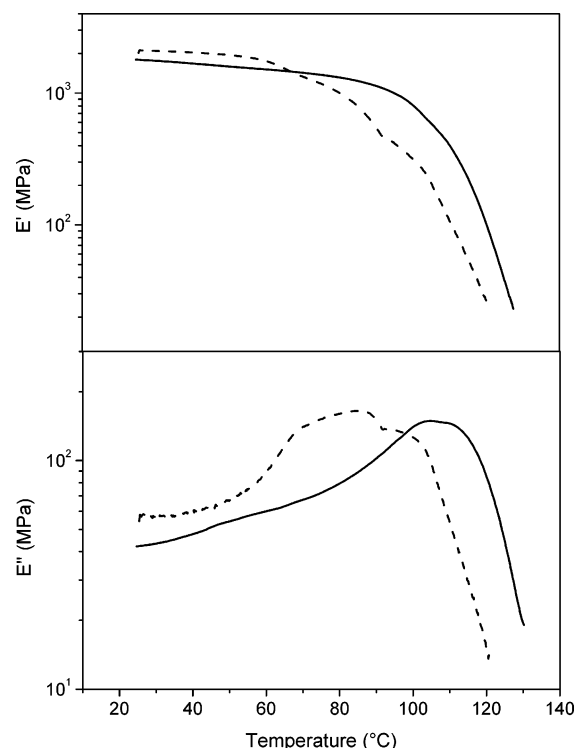


**Figure 4.** Temperature dependence of the storage ( $E'$ ) and loss ( $E''$ ) modulus of the copolymers (---) **PAE-g-PEO-3i** and (—) **FPAE-g-PEO-4**.

formation of two  $T_m$ 's indicated that two different crystal structures were present. The melting transitions at 55 °C was assigned to the crystalline structure of the ordered PEO-2000 side chain and the other one due to the presence of a population of smaller, less stable crystallites in the sample that melted at lower temperatures. Optical microscopy experiments for the same copolymer revealed the formation of spherulites which fill the whole sample.

On the other hand, copolymers **PAE-g-PEO-3i-3ii** and **FPAE-g-PEO-4** did not show any endothermic peak in the scanning range −50 to 250 °C, indicating that these copolymers have an amorphous structure. Thus, the absence of crystallization, which is a basic requirement for high conductivity in solid polymer electrolytes, depends strongly on copolymer composition.

The glass transition temperatures of the copolymers were determined with dynamic mechanical analysis (DMA). Generally, it was observed that the  $T_g$ 's of copolymers **PAE-g-PEO-3i-3iii** decreased with increasing PEO content. The temperature dependence of storage ( $E'$ ) and loss ( $E''$ ) modulus for copolymers **PAE-g-PEO-3i** and **FPAE-g-PEO-4** is shown in Figure 4. Careful examination of the  $E''$ – $T$  curve of copolymer **PAE-g-PEO-3i** revealed two broad overlapping peaks. The low-temperature broad peak could be attributed to the glass transition temperature of the PEO block, while the other peak around 100 °C to the glass transition temperature of the poly(arylene ether sulfone) block, respectively. In the case of copolymer **FPAE-g-PEO-4**, a broad peak corresponding to the  $T_g$  of copolymer was observed at higher temperatures (around 110 °C), mostly because of the increased stiffness of the decafluorobiphenyl backbone.

In the majority of current polymeric electrolytes, water is needed as the mobile phase to facilitate proton conductivity; thus, the proton transport properties are

strongly associated with the water uptake of the copolymer membrane. Table 3 shows the water uptake ability of copolymers **PAE-g-PEO-3** and **FPAE-g-PEO-4** for different temperatures. It is evident that as the temperature increased, copolymers showed a significantly improved water uptake behavior. Additionally, since the PEO units are hydrophilic, the water uptake of copolymers increased with increasing PEO content. Finally, copolymer **FPAE-g-PEO-4** cannot be impregnated with water even at 100 °C, due to the extreme hydrophobicity of decafluorobiphenyl unit.

The morphology of these copolymers has been investigated by scanning electron microscopy (SEM). An SEM micrograph of the cryogenic fracture of **PAE-g-PEO-3i** membrane is shown in Figure 5a. This copolymer which contains hydrophilic and hydrophobic units showed nanophase separation due to the mutual repulsion of the dissimilar blocks. In particular, the light gray circular domains, surrounded by dark gray domains, were regarded as spheres of the hydrophilic segments embedded in a hydrophobic matrix. The average size of the hydrophilic spheres was found to be 50–80 nm (Figure 5b). The observed morphology is quite similar to that of block copolymers containing hydrophobic and sulfonated hydrophilic blocks.<sup>32</sup>

Despite the fact that these copolymers were amorphous and exhibited good mechanical and thermal properties, the low water uptake was a limiting factor for the proton conductivity, and thus the system had to be modified. Water-soluble polymers with high PEO content were chosen to improve the water uptake behavior. Thus, to take advantage of the high water solubility of polymers **PES-g-PEO-1**, combined with the excellent thermal and mechanical properties of sulfonated polysulfone, which exhibits limited water uptake ability, binary blends were prepared and studied. Sulfonated polysulfone, as was mentioned in the Introduction, is one of the attractive polymer electrolytes for PEMFC.<sup>33</sup> Blends of sulfonated polysulfone with sulfonation degree 55% (SPSF(Na)<sub>55</sub>) and polymer **PES-g-PEO-1ii** at different compositions were studied, as shown in Table 4.

To investigate the phase behavior of the blends, dynamic mechanical analysis has been performed. The storage ( $E'$ ) and loss ( $E''$ ) moduli curves of neat sulfonated polysulfone and blend **B** as a function of temperature are given in Figure 6. Sulfonated polysulfone exhibited two glass transition temperatures. The broad peak at 210 °C was due to the glass transition of polysulfone matrix, while the sharp peak at 300 °C, corresponding to the glass transition of ionic clusters, was formed by aggregation of the sulfonate groups. This behavior was also observed with the related sulfonated poly(arylene ether sulfone) copolymers.<sup>12</sup> In the case of blend **B**, two broad overlapping peaks were observed at 215 and 185 °C. This behavior can be interpreted by considering ionomers mixed with polar or nonpolar plasticizers.<sup>34–36</sup> The higher temperature peak could be ascribed to the  $T_g$  of clusters, since PEO grafts of the polymer **PES-g-PEO-1ii** plasticized mainly the cluster regions of sulfonated polysulfone and thus caused a large decrease in the glass transition temperature of blend **B** compared to the corresponding one of neat sulfonated polysulfone. The  $T_g$  decrease is related to PEO, which resided in clusters and weakened ion interactions. The second peak of blend **B** at 185 °C could be attributed to the matrix  $T_g$ . The observed drop of  $T_g$

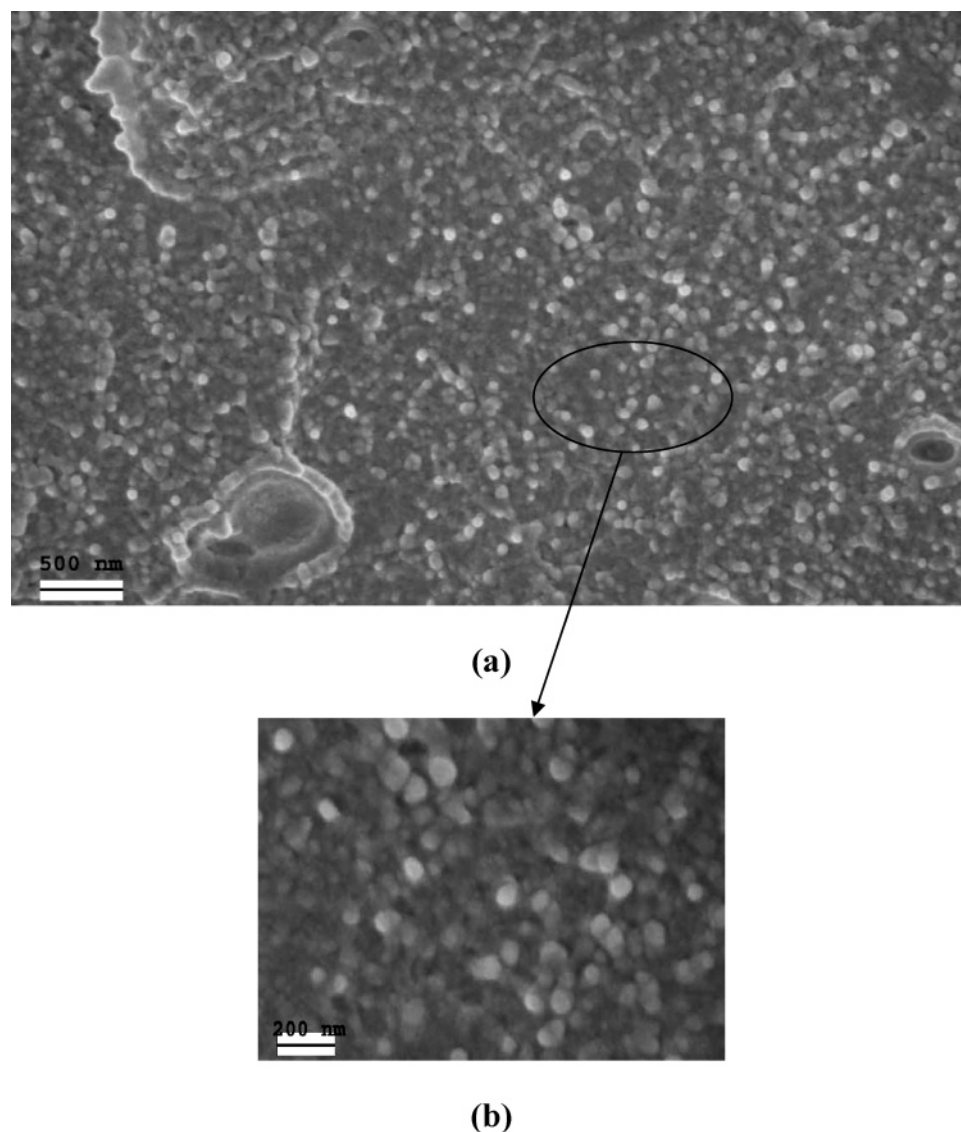


**Figure 5.** SEM images of the cryofractured surfaces of copolymer **PAE-g-PEO-3i**.

**Table 4. Composition and Water Uptake of SPSF(Na)<sub>55</sub>/PES-g-PEO-1ii Blend Membranes**

code	composition	water uptake (%)			
		20 °C <sup>a</sup>	70 °C <sup>a</sup>	85 °C <sup>a</sup>	100 °C <sup>b</sup>
SPSF(Na) <sub>55</sub> /PES-g-PEO-1ii	100/0	4	6	20	20 <sup>a</sup>
<b>A</b>	95/5	7	17	37	40
<b>B</b>	90/10	11	17	46	155
<b>C</b>	85/15	7	18	71	289

<sup>a</sup> Conducted at the desired temperatures for 24 h. <sup>b</sup> Conducted at 100 °C for 20 min.

could be ascribed to the reduction of the stiff sulfonated polysulfone backbone caused by the **PES-g-PEO-1ii** polymer. Further work is required to clarify the mechanism of the  $T_g$  reduction in blend **B**. Generally, it can be observed that in the temperature range relevant to fuel cell application, from 80 °C to well above 150 °C, the moduli of the blend remained at a rather high plateau values between  $10^3$  and  $10^2$  MPa, which are comparable to that of a stiff rubbery material.

To evaluate the water absorption and dimensional change of the hydrated blends, their water uptake was measured as a function of temperature, as is shown in Figure 7. Although the **PES-g-PEO-1ii** is water-soluble,

treatment of the membranes of blends with water did not remove this polymer which was trapped into the polysulfone matrix. Since PEO is a hydrophilic polymer, the water uptake of the blends increased with increasing the **PES-g-PEO-1ii** content. In particular, blend **A** has a water uptake around 37 wt % at 85 °C, a value that is approximately half of that obtained for blend **C** with the higher **PES-g-PEO-1ii** content. The dramatic effect of temperature on water uptake behavior is also illustrated in the same figure. Blends **B** and **C** exhibited a drastic increase in water uptake at 100 °C, reaching 155 and 289 wt % (it needed only 10 min to reach these values), respectively. In contrast, the neat sulfonated polysulfone reached a very low water uptake, about 20 wt %, at the same temperature.

These results showed that the water absorption of membranes from blends **B** and **C** increased linearly up to 70 °C and thereafter increased very rapidly. Nonlinear water uptake was also observed with the related sulfonated poly(arylene ether sulfone)<sup>12</sup> and sulfonated poly(arylene ether ketone)<sup>5</sup> systems. This high water absorption capacity may be suggestive of the presence of ion-rich regions where the ions aggregate together to form hydrophilic clusters. However, these highly hydrated membranes suffer from low mechanical strength



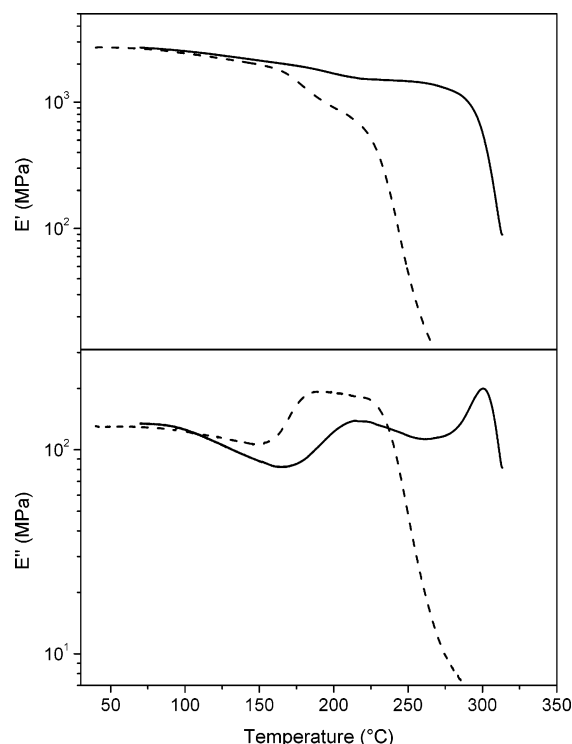


**Figure 6.** Temperature dependence of the storage ( $E'$ ) and loss ( $E''$ ) modulus of (—) SPSF(Na)<sub>55</sub> and blend (---) SPSF(Na)<sub>55</sub>/PES-g-PEO-1ii 90/10.

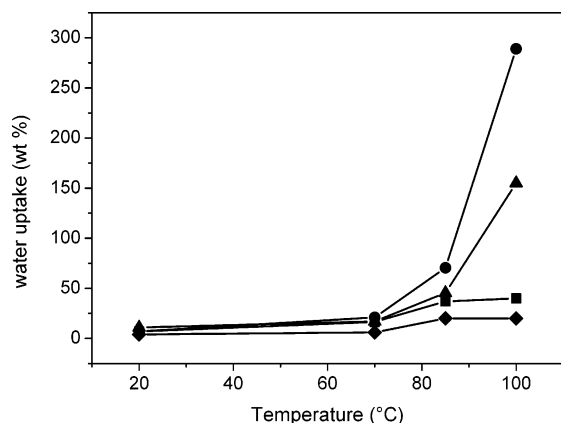
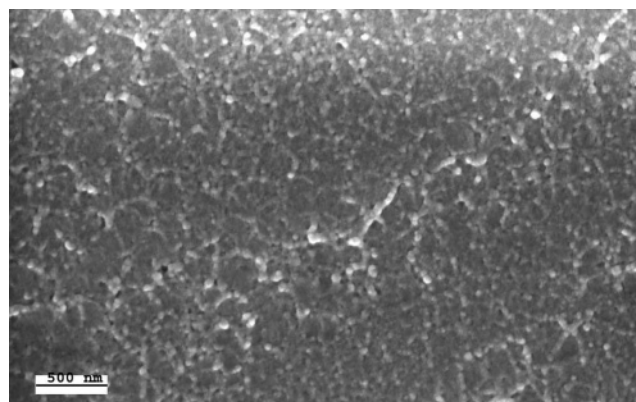


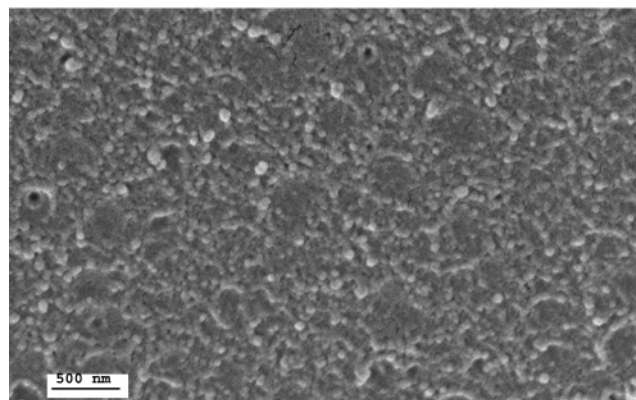
**Figure 7.** Influence of the temperature on the water uptake behavior of the blends: (◆) SPSF(Na)<sub>55</sub>/PES-g-PEO-1ii 100/0, (■) SPSF(Na)<sub>55</sub>/PES-g-PEO-1ii 95/5, (▲) SPSF(Na)<sub>55</sub>/PES-g-PEO-1ii 90/10, and (●) SPSF(Na)<sub>55</sub>/PES-g-PEO-1ii 85/15.

due to swelling. Thus, careful control of water uptake is required for reducing the adverse effects of swelling and degradation of the mechanical properties of the membrane in humid environments.

Since morphology plays an important role in determining the membrane properties such as the mechanical strength, water uptake, and proton conductivity, cryofractured surfaces of these blends have been studied by scanning electron microscopy. SEM micrographs of the cryogenic fracture of blend **B** and the same blend after treatment with water for 24 h and drying at room temperature are presented in Figure 8. The SEM image of blend membrane after water treatment (Figure 8b) did not show any holes, although polymer PES-g-PEO-1ii is water-soluble, confirming that no removal of the water-soluble component takes place. The surface showed nanophase separation which was more pronounced in the water treated surfaces. Spherical ionic domains



(a)



(b)

**Figure 8.** SEM images of the blend SPSF(Na)<sub>55</sub>/PES-g-PEO-1ii 90/10 (a) without any treatment, (b) after treatment with water.

(hydrophilic clusters) were uniformly distributed across the membrane and were embedded in the polysulfone hydrophobic matrix. The average size of the clusters was approximately 50–100 nm.

However, to examine whether the water-soluble component is leached from the blends with time in the presence of water, blend **B** was immersed in water for 5 days and then dried at room temperature. In this case, the SEM image of the cryogenic fracture of the treated blend (not shown) revealed the existence of holes with average diameter about 200 nm, indicating the partial removal of the water-soluble component with time.

Proton conductivities of the hydrated blend membranes were measured in a four-probe cell at room temperature. In Figure 9 the proton conductivity of the blend membrane **B** is compared with blend **C** as a function of water uptake. It can be seen that for almost the same water uptakes (127–128 wt %) blend **C** had a higher ionic conductivity, with a value of 0.004 S/cm at room temperature (65% relative humidity), which is 3 times higher compared to that of the corresponding blend **B**. This is related to the higher weight content of PES-g-PEO-1ii, resulting in improved proton conductivity of the blend **C**. The present materials could be applied as polymer electrolytes in fuel cells operating at low temperatures (80–100 °C), since combination of high ionic conductivity with easy preparation from inexpensive starting materials was achieved.

## Conclusions

Poly(arylene ether)s containing PEO side chains have been synthesized by direct aromatic nucleophilic sub-



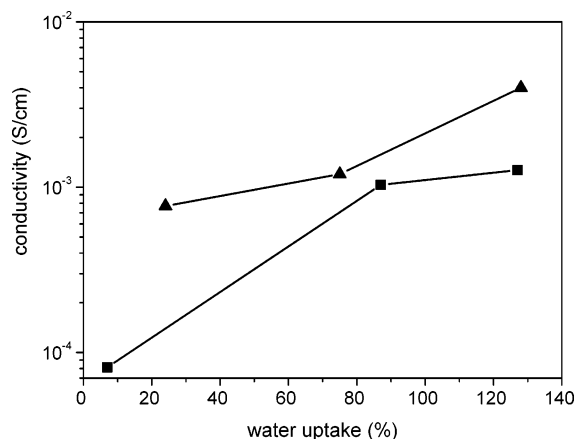


**Figure 9.** Conductivity of the blends (■) SPSF(Na)<sub>55</sub>/PES-g-PEO-1ii 90/10 and (▲) SPSF(Na)<sub>55</sub>/PES-g-PEO-1ii 85/15 as a function of water uptake.

stitution polycondensation of dihydroxy end-function-alized PEO, bisphenol A, and 4-fluorophenyl sulfone or decafluorobiphenyl. The copolymers exhibited film-forming ability, high thermal stability, good mechanical properties, and amorphous structures in most cases. Blends of sulfonated polysulfone and water-soluble PES-g-PEO polymers were prepared in order to improve the water uptake ability. Flexible blend membranes were obtained by solution casting. Blend membranes presented high glass transition temperatures, as revealed by dynamic mechanical analysis. SEM study showed that hydrophilic spherical clusters with a diameter of 50–100 nm were formed. The water uptake of the membranes was greatly influenced by temperature and PES-g-PEO weight content. The blend with the higher PES-g-PEO content showed a proton conductivity value of  $4 \times 10^{-3}$  S/cm at room temperature. The ionic conductivity was strongly dependent on the water uptake and PES-g-PEO content. Further research on high-temperature conductivity and fuel cell performance of these materials is in progress.

**Acknowledgment.** We thank the European Social Fund (ESF), Operational Program for Educational and Vocational Training II (EPEAEK II), and particularly the program PYTHAGORAS, for funding the above work. The authors are indebted to Dr. V. Dracopoulos (FORTH/ICEHT) for his help in SEM measurements.

## References and Notes

- (1) Steele, B. C. H.; Heinzel, A. *Nature (London)* **2001**, *414*, 345–352.
- (2) Hickner, M. A.; Ghassemi, H.; Kim, Y. S.; Einsla, B. R.; McGrath, J. E. *Chem. Rev.* **2004**, *104*, 4587–4612.
- (3) Bishop, M. T.; Karasz, F. E.; Russo, P. S.; Langley, K. H. *Macromolecules* **1985**, *18*, 86–93.
- (4) Roziere, J.; Jones, D. J. *Annu. Rev. Mater. Res.* **2003**, *33*, 503–555.
- (5) Zaidi, S. M. J.; Mikhailenko, S. D.; Robertson, G. P.; Guiver, M. D.; Kaliaguine, S. *J. Membr. Sci.* **2000**, *173*, 17–34.
- (6) Kreuer, K. D. *J. Membr. Sci.* **2001**, *185*, 29–39.
- (7) Robertson, G. P.; Mikhailenko, S. D.; Wang, K.; Xing, P.; Guiver, M. D.; Kaliaguine, S. *J. Membr. Sci.* **2003**, *219*, 113–121.
- (8) Noshay, A.; Robeson, L. M. *J. Appl. Polym. Sci.* **1976**, *20*, 1885–1903.
- (9) Johnson, B. C.; Yilgor, I.; Tran, C.; Iqbal, M.; Wightman, J. P.; Lloyd, D. R.; McGrath, J. E. *J. Polym. Sci., Polym. Chem. Ed.* **1984**, *22*, 721–737.
- (10) Kerres, J. *J. Membr. Sci.* **2001**, *185*, 3–27.
- (11) Nolte, R.; Ledjeff, K.; Bauer, M.; Mulhaupt, R. *J. Membr. Sci.* **1993**, *83*, 211–220.
- (12) Wang, F.; Hickner, M.; Kim, Y. S.; Zawodzinski, T. H.; McGrath, J. E. *J. Membr. Sci.* **2002**, *197*, 231–242.
- (13) Meyer, W. H. *Adv. Mater.* **1998**, *10*, 439–448.
- (14) Berthier, C.; Gorecki, W.; Minier, M.; Armand, M.; Chabagno, J.-M.; Rigaud, P. *Solid State Ionics* **1983**, *11*, 91–95.
- (15) Watanabe, M.; Nagano, S.; Sanui, K.; Ogata, N. *Solid State Ionics* **1986**, *18/19*, 338–342.
- (16) Lascaud, S.; Perrier, M.; Vallee, A.; Besner, S.; Prud'homme, J.; Armand, M. *Macromolecules* **1994**, *27*, 7469–7477.
- (17) Tarascon, J. M.; Armand, M. *Nature (London)* **2001**, *414*, 359–367.
- (18) Bannister, D. J.; Davies, G. R.; Ward, I. M.; McIntyre, J. E. *Polymer* **1984**, *25*, 1600–1602.
- (19) Blonsky, P. M.; Shriver, D. F.; Austin, P.; Allock, H. R. *J. Am. Chem. Soc.* **1984**, *106*, 6854–6855.
- (20) Qiao, J.; Yoshimoto, N.; Ishikawa, M.; Morita, M. *Chem. Mater.* **2003**, *15*, 2005–2010.
- (21) Jannasch, P. *Macromolecules* **2000**, *33*, 8604–8610.
- (22) Nagaoka, K.; Naruse, H.; Shinohara, I.; Watanabe, M. *J. Polym. Sci., Polym. Lett. Ed.* **1984**, *22*, 659–663.
- (23) Soo, P. P.; Huang, B.; Jang, Y.-I.; Chiang, Y.-M.; Sadoway, D. R.; Mayes, A. M. *J. Electrochem. Soc.* **1999**, *146*, 32–37.
- (24) Gray, F. M.; MacCallum, J. R.; Vincent, C. A. *Solid State Ionics* **1986**, *18/19*, 282–286.
- (25) Li, J.; Khan, I. M. *Macromolecules* **1993**, *26*, 4544–4550.
- (26) Chiu, C.-Y.; Chen, H.-W.; Kuo, S.-W.; Huang, C.-F.; Chang, F.-C. *Macromolecules* **2004**, *37*, 8424–8430.
- (27) Deimede, V.; Kallitsis, J. K. *Chem.-Eur. J.* **2002**, *8*, 467–473.
- (28) Deimede, V.; Voyiatzis, G. A.; Kallitsis, J. K.; Qingfeng, L.; Bjerrum, N. J. *Macromolecules* **2000**, *33*, 7609–7617.
- (29) Ghosh, B. D.; Lott, K. F.; Ritchie, J. E. *Chem. Mater.* **2005**, *17*, 661–669.
- (30) Cianga, L.; Sarac, A.; Ito, K.; Yagci, Y. *J. Polym. Sci., Part A: Polym. Chem.* **2005**, *43*, 479–492.
- (31) Iyer, J.; Fleming, K.; Hammond, P. T. *Macromolecules* **1998**, *31*, 8757–8765.
- (32) Shin, C. K.; Maier, G.; Andreaus, B.; Scherer, G. G. *J. Membr. Sci.* **2004**, *245*, 147–161.
- (33) Lufrano, F.; Squadrito, G.; Patti, A.; Passalacqua, E. *J. Appl. Polym. Sci.* **2000**, *77*, 1250–1256.
- (34) Eisenberg, A.; Hird, B.; Moore, R. B. *Macromolecules* **1990**, *23*, 4098–4107.
- (35) Kim, J.-S.; Jackman, R. J.; Eisenberg, A. *Macromolecules* **1994**, *27*, 2789–2803.
- (36) Kim, J.-S.; Hong, M.-C.; Nah, Y. H. *Macromolecules* **2002**, *35*, 155–160.

MA050615M